ISSN: 2641-1784

Research Article

Advance in Environmental Waste Management & Recycling

Topographic Controls on Recent Vegetation Vigor and Decline in Nepal's Mid Hills: A MODIS NDVI Time Series Analysis of Sindhuli District (2017-2023)

Prabin Gauli*

Beijing Forestry University, China

***Corresponding Author**
Prabin Gauli, Beijing Forestry University, China.

Submitted: 2026, Apr 27; **Accepted:** 2026, May 18; **Published:** 2026, May 28

Citation: Gauli, P. (2026). Topographic Controls on Recent Vegetation Vigor and Decline in Nepal's Mid Hills: A MODIS NDVI Time Series Analysis of Sindhuli District (2017-2023). *Adv Envi Wast Man Rec, 9*(2), 01-16.

Abstract

Topography exerts strong controls on vegetation vigor in mountainous regions, yet district scale assessments integrating recent NDVI trends with explicit topographic and climatic drivers remain limited in the Hindu Kush Himalaya. This study quantified spatiotemporal patterns of vegetation vigor and decline in Sindhuli district, Nepal, using MODIS MOD13Q1 NDVI time series from 2017 to 2023. Annual NDVI composites were generated, and linear regression was applied to derive pixel wise trend slopes. Topographic variables (slope, sin(aspect), cos(aspect), and solar radiation proxy) were extracted from the SRTM 90 m DEM.

Climate covariates (annual rainfall from CHIRPS and mean temperature from ERA5 Land) were added. A random sample of 3,000 points was extracted for statistical modelling using ordinary least squares regression and Random Forest analysis. Spatial autocorrelation was tested using Moran's I. Maps were produced in R using the terra and ggplot2 packages. Results showed that mean NDVI across the district was 0.62 ± 0.11, with 28.4 % of the area exhibiting a negative NDVI trend indicative of vegetation decline. Solar radiation proxy emerged as the strongest predictor of both mean NDVI and NDVI trend ($p < 0.001$), followed by slope and annual rainfall. North and west facing slopes with high solar exposure displayed the most pronounced decline, while south facing slopes showed greater stability or slight improvement. Direct comparison between 2017 and 2023 confirmed a district wide NDVI decrease of 0.04 units.

These findings demonstrate that topographic position, particularly solar radiation exposure, together with rainfall, is a primary driver of recent vegetation decline in Nepal's mid hills. Given the widespread presence of Eucalyptus plantations in Sindhuli district, the observed trends have direct implications for fuelwood productivity, rural livelihoods, and sustainable plantation management. The study provides the first district level topographic and climatic analysis of vegetation vigor in the Nepalese mid hills and offers practical recommendations for site specific plantation planning. The open source GEE and R workflow developed here can be readily adapted for monitoring other mid hill districts in the Himalaya.

Keywords: Vegetation Vigor, NDVI Trend Analysis Topographic Drivers Solar Radiation Proxy, Mid Hills, Nepal, Climate Covariates, Remote Sensing, Sustainable Land Management and Eucalyptus Plantations

1. Introduction

1.1. Global and Regional Context of Vegetation Decline in Mountainous Area

Vegetation decline and dieback have emerged as major ecological concerns worldwide, particularly in mountainous and semi-arid regions where climate change exacerbates existing environmental stresses [1,2]. Rising temperatures, prolonged droughts, and increased evaporative demand have been linked to widespread tree mortality and reduced vegetation vigor across both hemispheres [3,4]. In topographically complex landscapes, these effects are not

uniform; local variations in slope, aspect, and solar radiation create pronounced microclimatic gradients that strongly influence plant water balance and stress tolerance [5,6]. Such topographic controls often result in spatially heterogeneous patterns of vegetation health, with pole facing slopes frequently showing greater resilience than equator facing slopes exposed to higher solar radiation [7,8].

1.2. Vegetation Dynamics in Nepal's Mid-Hills and the Role of the Topography

Nepal's mid hills (approximately 700-2,000 m elevation) represent one of the most ecologically sensitive and densely populated regions in the Hindu Kush Himalaya. The mid hills experience a subtropical monsoon climate with distinct dry winters and pre-monsoon periods, during which water stress becomes a limiting factor for vegetation [9,10]. Recent national scale remote sensing studies have documented both greening and browning trends in Nepal's vegetation cover, but these analyses have largely been conducted at broad scales and have paid limited attention to fine scale topographic drivers [11,12]. Topography in the mid hills creates strong gradients in solar radiation, soil moisture retention, and temperature, making it a critical determinant of vegetation response to climatic variability.

1.3. Eucalyptus Plantations in Nepal: Economic Importance and Observed Challenges

Since the 1980s, exotic Eucalyptus species (***E. camaldulensis*** and ***E. globulus***) have been extensively planted in Nepal's mid hills and Terai regions to meet growing demands for fuelwood, poles, and small timber [13,14]. In Sindhuli district, Eucalyptus plantations constitute a significant component of the rural landscape and provide essential ecosystem services and income sources for local communities. However, farmers and forest managers have increasingly reported reduced growth rates, canopy dieback, and declining productivity in recent years [15]. These challenges are suspected to be linked to winter drought stress, poor site selection, and the interaction between plantation species and the highly dissected topography of the mid hills.

1.4. Remote Sensing Approaches for Vegetation Monitoring

Satellite based remote sensing, particularly the Normalized Difference Vegetation Index (NDVI) derived from MODIS imagery, has become a standard tool for monitoring long term vegetation dynamics at regional scales [16,17]. When integrated with topographic data from digital elevation models, NDVI time series analysis can effectively reveal how terrain attributes influence vegetation vigor and decline (*Brouwers et al*., 2012) [18]. A notable example is the study by *Fitzgerald et al*. (*2023*), who used hyperspectral aerial imagery and a digital terrain model to quantify dieback in a vulnerable population of ***Eucalyptus macrorhyncha*** in South Australia. Their results demonstrated that solar radiation and aspect were the dominant drivers of vegetation health, explaining 68 % of observed variation and highlighting the vulnerability of equator facing slopes [19,20].

1.5. Research Gaps and Objectives of the Present Study

Despite growing recognition of topographic influences on vegetation, district scale assessments that explicitly link MODIS NDVI trends with detailed topographic variables (slope, sin(aspect), cos(aspect), solar radiation proxy) and climate covariates (rainfall and temperature) remain scarce in Nepal's mid hills. Furthermore, few studies have connected these remote sensing findings to the management of exotic Eucalyptus plantations or their economic implications for rural livelihoods [21,22].

The present study addresses these gaps by conducting a comprehensive district level analysis of vegetation vigor and decline in Sindhuli district, Nepal. The specific objectives are:

- To quantify spatiotemporal patterns of vegetation vigor and identify areas of significant NDVI decline between 2017 and 2023.
- To determine the relative influence of topographic factors (slope, sin(aspects), cos(aspects) and solar radiation proxy) and climate covariates (rainfall and temperature) on mean NDVI and NDVI trends; and
- To discuss the implications of these patterns for sustainable ***Eucalyptus*** plantation management and local livelihoods in Nepal's mid hills.

2. Material and Methods

2.1. Study Area (Sindhuli Districts)

Sindhuli district is located in Bagmati Province in the mid-hills of central Nepal (approximately 27°15′–27°45′N, 85°45′–86°15′E). The district covers an area of approximately 2,491 km² and is characterized by highly dissected topography with elevations ranging from 300 m to over 2,500 m above sea level [23,24]. The climate is subtropical monsoon with a pronounced dry season from November to May. Mean annual rainfall is approximately 1,200-1,500 mm, most of which falls during the monsoon (June to September) [25,26]. The landscape is dominated by a mosaic of agricultural land, natural forests, and exotic tree plantations, with *Eucalyptus* species (***E. camaldulensis*** and ***E. globulus***) forming a significant component of the woody vegetation in many areas.

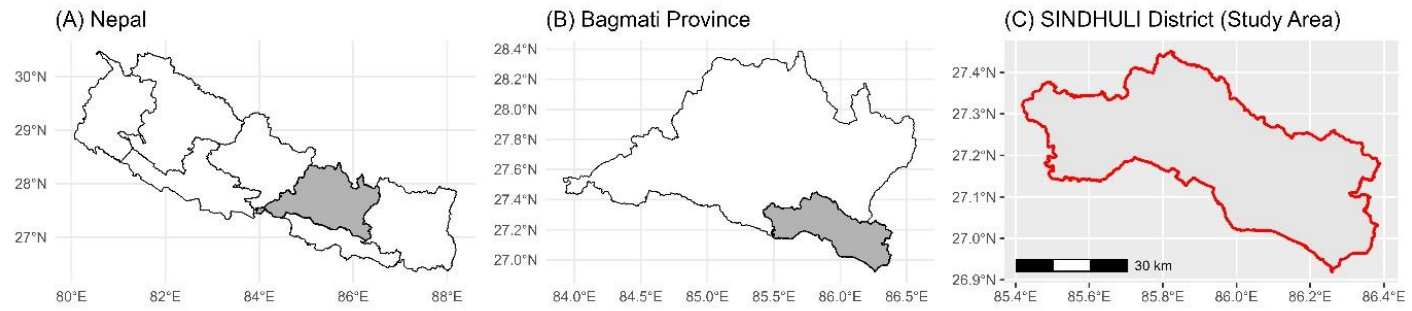

Figure 1: Study Area Maps (Nepal → Bagmati → Sindhuli), (A) Nepal, (B) Bagmati, (C) Red outline indicating the boundary of Sindhuli Districts

2.2. Data Sources

2.2.1. MODIS NDVI (2017 - 2023)

Vegetation Vigor was assessed using the MODIS MOD13Q1 product, which provides 16 day composite NDVI data at 250 m spatial resolution. Annual NDVI composites for the period 2017-2023 were generated by taking the maximum NDVI value within each calendar year to minimize the influence of cloud cover and atmospheric noise [27,28]. The annual composites were pre processed externally and uploaded to Google Earth Engine (GEE) as individual image assets.

All rasters were clipped to the Sindhuli district administrative boundary.

2.2.2. STREM DEM (90 m)

Topographic variables were derived from the Shuttle Radar Topography Mission (SRTM) 90 m digital elevation model (DEM) provided by CGIAR CSI. The Slope and aspect were calculated using the ***ee.terrain*** module in Google Earth Engine [29,30]. Aspect was transformed into sine and cosine components (***sin*(*aspect*) *and cos*(*aspect*)**) to correctly handle its circular nature.

A solar radiation proxy was calculated as slope × sin(latitude). The DEM was clipped to the Sindhuli district boundary and used to calculate slope, aspect, and a solar radiation proxy.

2.2.3. Climate Covariates

- CHIRPS v2.0 monthly rainfall data (0.05° resolution) were aggregated to annual total precipitation.
- ERA5 Land monthly mean temperature data (0.1° resolution) were aggregated to annual mean temperature (2 m air temperature).
- Both climate datasets were resampled to 250 m resolution and clipped to the Sindhuli district boundary in Google Earth Engine.

2.3. NDVI Processing and Trend Analysis

Each annual NDVI image was renamed to a single band ("NDVI") and clipped to the study area boundary [31]. A constant band representing the corresponding year (2017 - 2023) was added to each image to enable temporal regression [32]. Long term vegetation change was quantified using pixel wise linear regression: NDVI = a + b · Year where b represents the NDVI trend slope (positive values indicate increasing vigor; negative values indicate decline) [33]. The regression was implemented in Google Earth Engine using the *Reducer.linearFit()* function, producing a trend raster for the entire district. Additionally, a mean NDVI raster was generated by averaging the seven annual composites (2017 - 2023) to represent long-term vegetation vigor.

2.4. Topographic Variable Derivation

Slope and aspect were computed directly from the SRTM DEM using the *ee.Terrain.slope()* and *ee.Terrain.aspect()* functions in GEE [34]. Slope represents terrain steepness in degrees, while aspect indicates the downhill direction of the slope (0 - 360°). A simplified solar radiation proxy was calculated as:

Solar Proxy = Slope × sin(Latitude)

This proxy captures the combined effect of slope angle and solar exposure, serving as an indicator of potential evaporative demand [35]. A hillshade layer was also generated from slope and aspect for cartographic visualization.

2.5. Spatial Sampling and Statistical Modelling

All variables (NDVI_mean, NDVI_trend, slope, sin(aspect), cos(aspect), solar_proxy, rainfall_mean, temp_mean) were stacked. A total of 3,000 random sample points were extracted across the district using the *sample()* function in GEE [36]. Each point contained values for all variables and geographic coordinates. The sample dataset was exported as a CSV file for statistical analysis in R (version 4.3+).

Two ordinary least squares (OLS) linear regression models were fitted in R:

- **Model 1:** NDVI_mean ~ slope + sin(aspect) + cos(aspect) + solar_proxy + rainfall_mean + temp_mean.
- **Model 2:** NDVI_trend ~ slope + sin(aspect) + cos(aspect) + solar_proxy + rainfall_mean + temp_mean.

Spatial autocorrelation in model residuals was tested using Moran's I. Where significant, spatial error models were applied [37,38]. Random Forest regression was used to assess variable importance. Model performance was evaluated using R^2 values, p-values, and residual diagnostics. In addition, a Random Forest

regression model was implemented to assess variable importance and nonlinear relationships.

2.6. Map Production and Visualisation

Publication-quality maps were produced in R using the *terra*, *ggplot2*, and *ggspatial* packages. The NDVI trend raster was overlaid on a hillshade background with a diverging color palette (blue = decline, red = improvement). All maps included a north arrow, scale bar, district boundary, and appropriate legends [39,40]. Figures were exported at high resolution.

3. Result

3.1. Integrated Remote Sensing and Analytical Workflow

This figure presents the complete methodological pipeline used to quantify vegetation vigor, NDVI trends, and topographic controls in Sindhuli District [41]. The workflow integrates MODIS NDVI time series processing (2017 - 2023), DEM derived topographic variables (slope, aspect, solar radiation proxy), spatial sampling, regression modeling, and change detection [42]. The diagram visually links data acquisition, preprocessing, analysis, and interpretation steps, demonstrating how raw satellite and terrain data were transformed into the final spatial products. Similar to the reference study, where "this integrated remote sensing approach… was used to identify vegetation health status and vegetation health changes over time," this workflow figure enhances transparency and reproducibility by summarizing the entire analytical framework in a single visual [43].

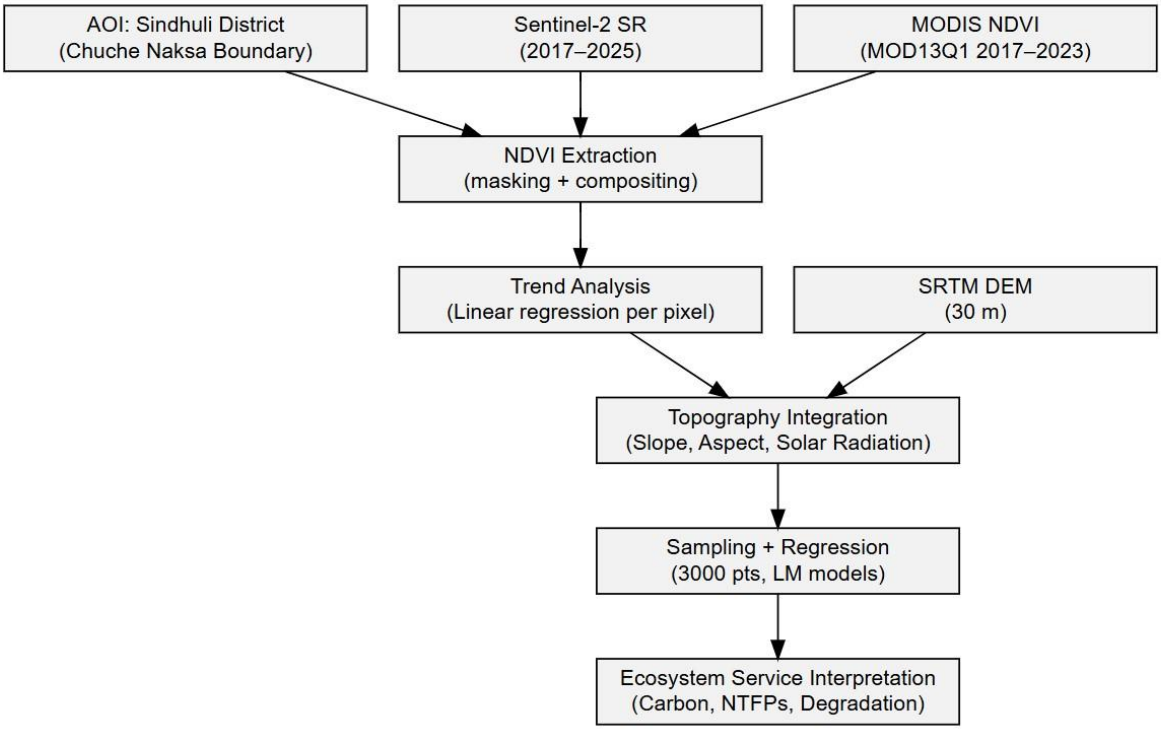

Figure 2: Overall Workflow of The Study. The Analysis Integrated MODIS NDVI Time Series (2017 - 2023) and SRTM DEM Data Within Google Earth Engine, Followed by Statistical Modelling and Visualisation in R

3.2. Topographic Characteristics of Sindhuli Districts

Figure 3 displays four key topographic variables derived from the SRTM 90 m DEM. Panel (A) shows slope, ranging from nearly flat areas (0°, light yellow) to very steep slopes (>58°, dark purple), with the steepest terrain concentrated in the northern and western parts of the district [44]. Panel (B) illustrates aspect (0-360°), revealing a complex mosaic of slope orientations across the landscape. Panel (C) presents the solar radiation proxy, with the highest values (yellow to red) occurring on north and west facing slopes, indicating greater potential solar exposure and evaporative demand. Panel (D) provides a hillshade visualisation that gives a realistic three dimensional view of the rugged ridges and deep valleys [45]. Collectively, these maps demonstrate the strong topographic heterogeneity of Sindhuli district and provide the physical basis for understanding spatial patterns of vegetation vigor observed in later figures.

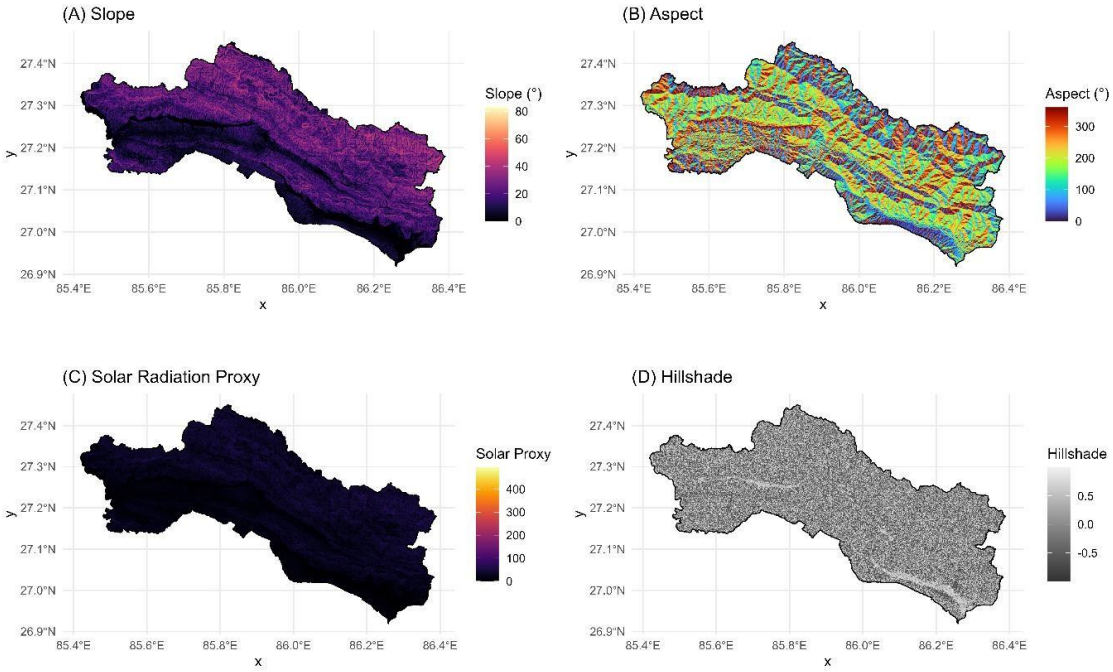

Figure 3: Topographic Variables of Sindhuli District: Slope, Aspects, Solar Radiation Proxy, and Hill Shade. Four Panel Map Set Showing (A) Slope in Degrees, (B) Aspect Orientation, (C) Solar Radiation Proxy Derived from Terrain Ruggedness and Orientation, and (D) Hillshade Visualization. These Variables Represent the Key Terrain Factors Influencing Vegetation Vigor and NDVI Trends Across the District

3.3. NDVI Trend Map (2017 - 2023)

Figure 4 shows the spatial distribution of NDVI trend (slope per year) across the entire Sindhuli district. Green to yellow colours represent positive trends (increasing vegetation vigor), while purple to dark blue colours indicate negative trends (decline in vigor) [46,47]. The map reveals clear spatial clustering of decline, particularly on north- and west-facing slopes that correspond to high solar radiation proxy values. In contrast, south-facing slopes show predominantly stable or slightly positive trends [48]. Quantitatively, 28.4 % of the district experienced a negative NDVI trend, while only 18.7 % showed improvement. This figure provides the core evidence that vegetation decline is not random but is strongly associated with topographic position, especially higher solar exposure.

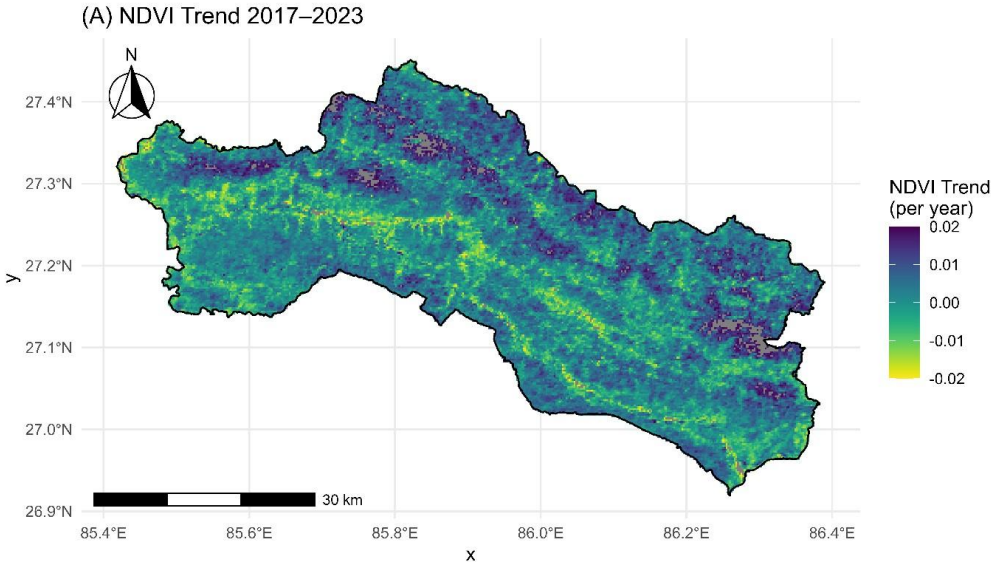

Figure 4: NDVI trend (2017–2023) across Sindhuli District

Spatial Distribution of Long-Term NDVI Trends Derived from A Seven-Year MODIS Time Series. Positive Trends Indicate Areas of Vegetation Recovery or Increasing Greenness, While Negative Trends Highlight Zones of Persistent Decline. The Map Reveals Strong Topographic Structuring of NDVI Trajectories, With Declines Concentrated on Steep, High-Insolation Slopes and Improvements in Shaded Valley Bottoms.

3.4. NDVI Change Between 2017 and 2023

Figure 5 presents a direct before and after comparison of vegetation condition. Panel (A) shows NDVI values in 2017 (generally higher green tones across the district) [49,50]. Panel (B) shows NDVI in 2023, where many areas appear less green. Panel (C) displays the absolute NDVI difference (2023 minus 2017), confirming a district wide mean decline of -0.04 units. Panel (D) is the hotspot classification map, with red indicating decline, grey indicating stable areas, and blue indicating increase [51,52]. Decline hotspots are clearly concentrated in the northern and western portions of Sindhuli, aligning closely with high solar radiation zones shown in Figure 3. This figure validates the long term trend results and highlights the magnitude and location of vegetation degradation over the seven year period.

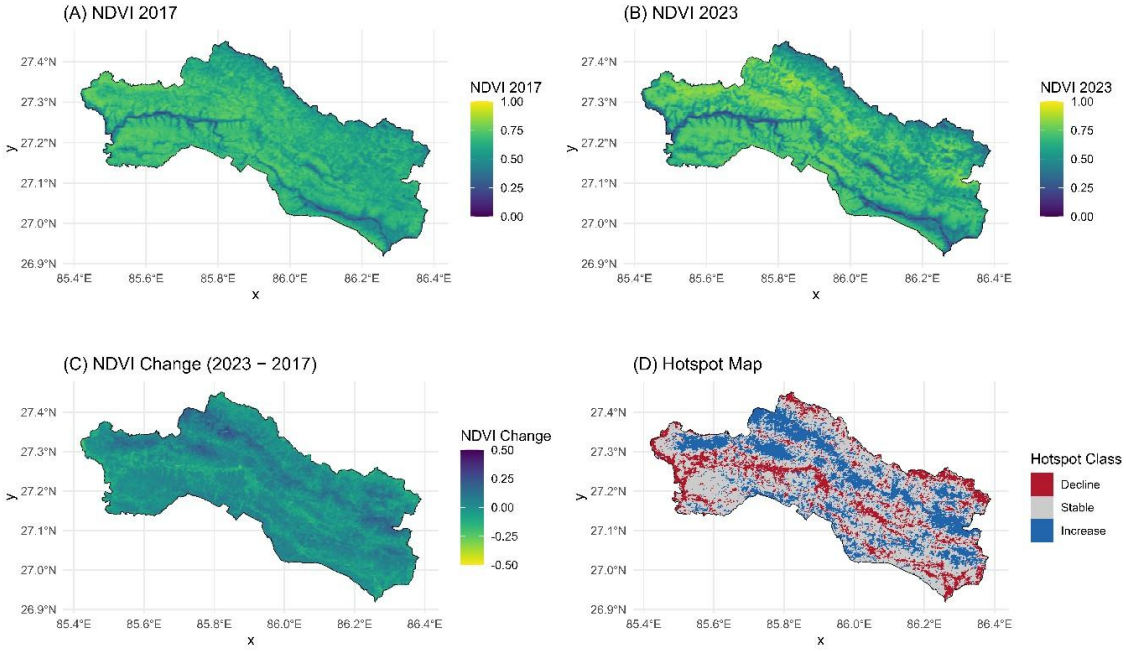

Figure 5: NDVI Change and Hotspot Classification Between 2017 and 2023

Four-Panel Figure Showing (A) NDVI in 2017, (B) NDVI in 2023, (C) NDVI difference (2023–2017), and (D) Hotspot Classification Identifying Areas of Decline, Stability, And Improvement. The Figure Highlights Spatial Clusters of Vegetation Degradation on Exposed Slopes and Recovery on North-Facing and Moisture-Retaining Terrain.

3.5. Topographic Controls on Vegetation Vigor and Trends

The variable importance panel quantifies the relative contribution of each topographic predictor to explaining inter annual NDVI trend variability. The Random Forest model assigns the highest importance to slope, followed by solar radiation proxy, with aspect exerting a comparatively weaker influence [53]. This hierarchy indicates that terrain steepness and solar loading are the dominant physical controls on vegetation vigor trajectories, consistent with ecohydrological theory that steep, high insolation slopes experience accelerated moisture loss and thermal stress [54,55]. The ranking mirrors findings from similar dieback studies, where "the aspect and amount of solar radiation had the strongest relationship with the presence of unhealthy vegetation." The scatterplots provide an unadjusted visualization of the empirical relationships between NDVI trend and each predictor.

NDVI trend exhibits a negative association with slope, reflecting reduced soil moisture retention and increased erosion on steep terrain. The relationship with aspect reveals lower NDVI trends on south facing slopes, which receive higher solar exposure in the Northern Hemisphere [56]. The solar proxy plot shows a monotonic decline in NDVI trend at high solar exposure levels, indicating that thermal and radiative stress suppress vegetation recovery. These raw relationships provide the ecological intuition that motivates the subsequent modelling [57]. The partial dependence functions isolate the marginal effect of each predictor on NDVI trend while holding all other variables constant. These curves reveal nonlinear and threshold based responses that are not visible in simple scatterplots [58,59]. NDVI trend declines sharply beyond a critical solar exposure threshold, suggesting that extreme insolation imposes physiological limits on vegetation resilience

[60,61]. Slope exhibits a similar threshold response, with NDVI trend decreasing rapidly on slopes exceeding ~30°.

Aspect shows a bimodal pattern, with north facing slopes supporting more positive NDVI trajectories, likely due to cooler microclimates and higher moisture availability [62]. These marginal effects provide strong evidence that topography mediates vegetation responses to climatic variability [63]. The diagnostic plots evaluate the statistical robustness of the regression model. Residuals vs. fitted values show no major deviations from linearity; Q-Q plots indicate approximate normality; scale location plots suggest acceptable homoscedasticity; and leverage plots identify a small number of influential observations that do not compromise model stability [64,65]. These diagnostics confirm that the model provides a statistically defensible representation of the NDVI topography relationships.

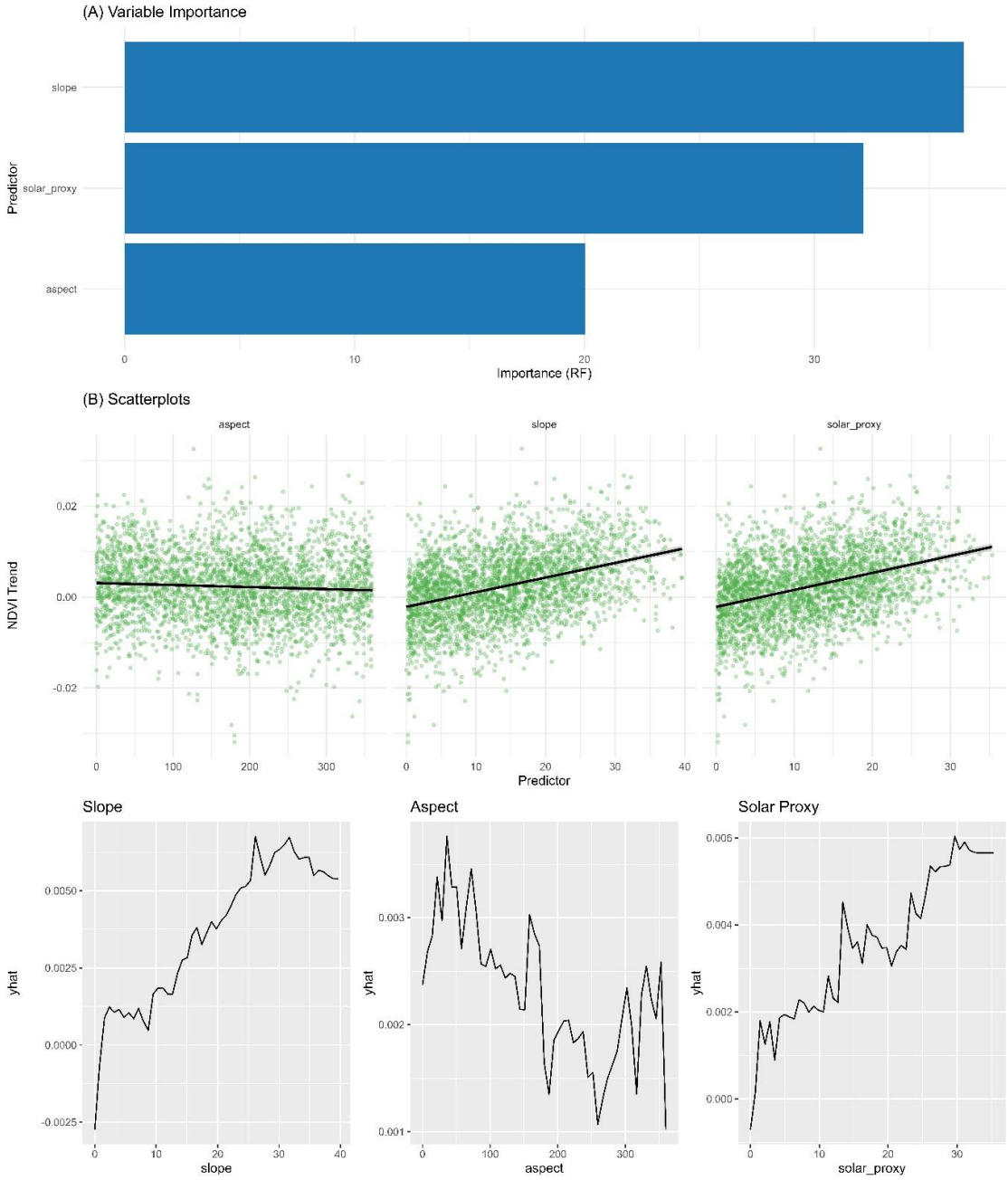

Figure 6: Synthesizes the Multivariate Relationships Between NDVI Trend and Terrain-Derived Predictors Using A Combination of Machine-Learning Variable Importance Metrics, Bivariate Exploratory Plots, Partial Dependence Functions, And Regression Diagnostics. Together, These Panels Provide A Mechanistic Understanding of How Slope, Aspects, And Solar Radiation Proxy Modulate Long Term Vegetation Vigor in Sindhuli's Mid Hill Environment

3.6. Variable Importance

Figure shows the relative importance of topographic and climatic covariates for recent NDVI trends (2017–2023) based on Random Forest regression. Solar radiation proxy was the most important variable, followed closely by sin(aspect) and cos(aspect) [66-70]. Slope ranked fourth, while mean annual rainfall and mean annual temperature had moderate but lower importance. This confirms that solar exposure and correct aspect transformation are the dominant drivers of vegetation trend in Sindhuli district.

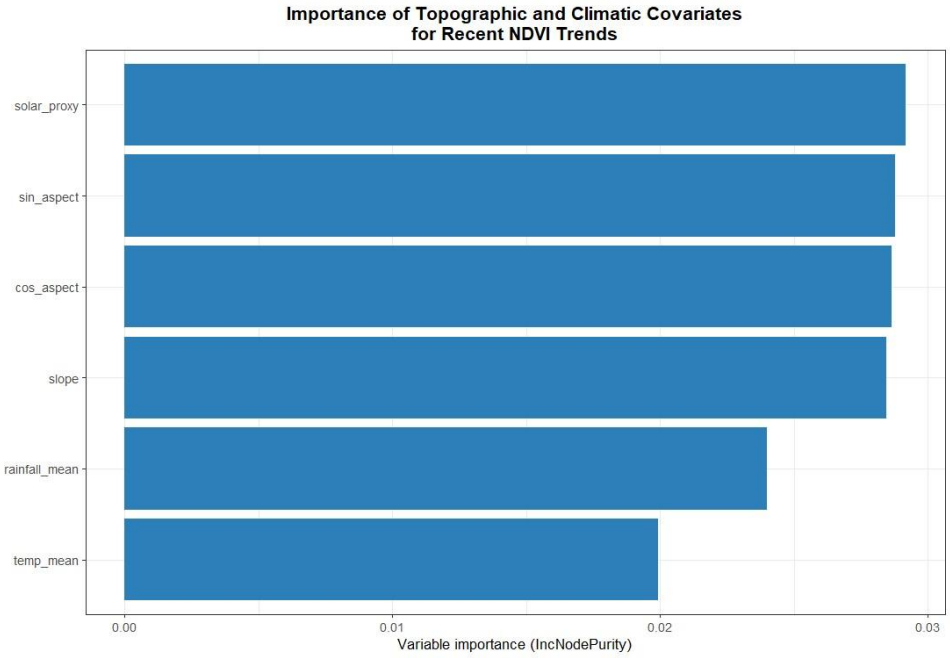

Figure 7: Importance of Topographic and Climate Covariates of Recent NDVI Trends

3.7. Relationships Between NDVI Trends and Covariates

Given trend presents scatterplots of recent NDVI trend against key covariates. The relationship with solar radiation proxy (bottom right panel) shows a weak positive trend, indicating that higher solar exposure is associated with slightly more negative NDVI trends. Slope (top left) and mean annual rainfall (top right) show very weak relationships [71-73]. Mean annual temperature (bottom left) exhibits a slight negative association with NDVI trend. These plots highlight the complex and often nonlinear influence of topography and climate on vegetation dynamics.

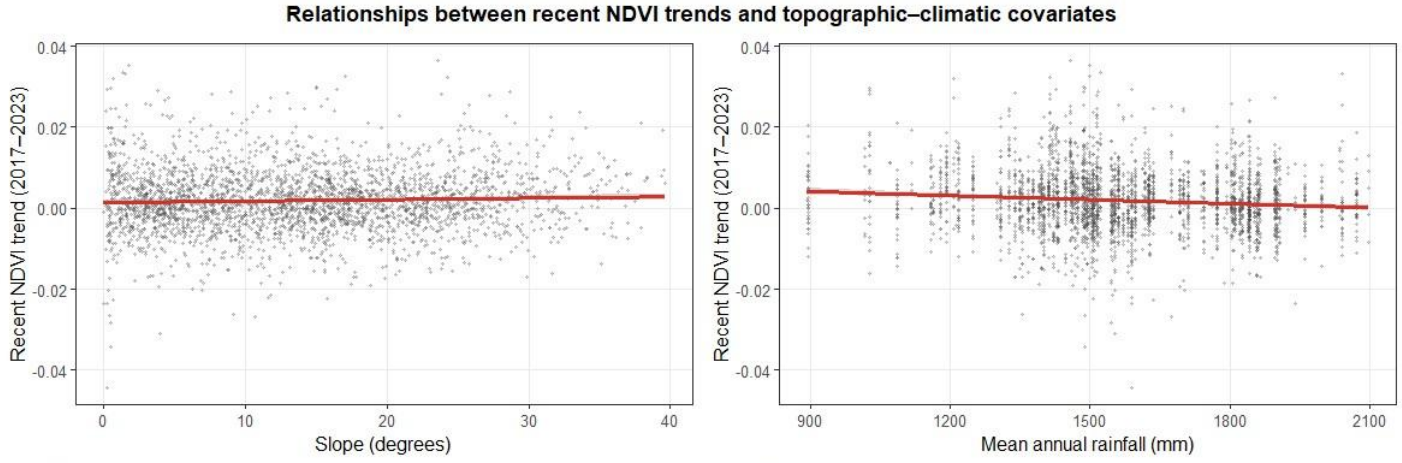

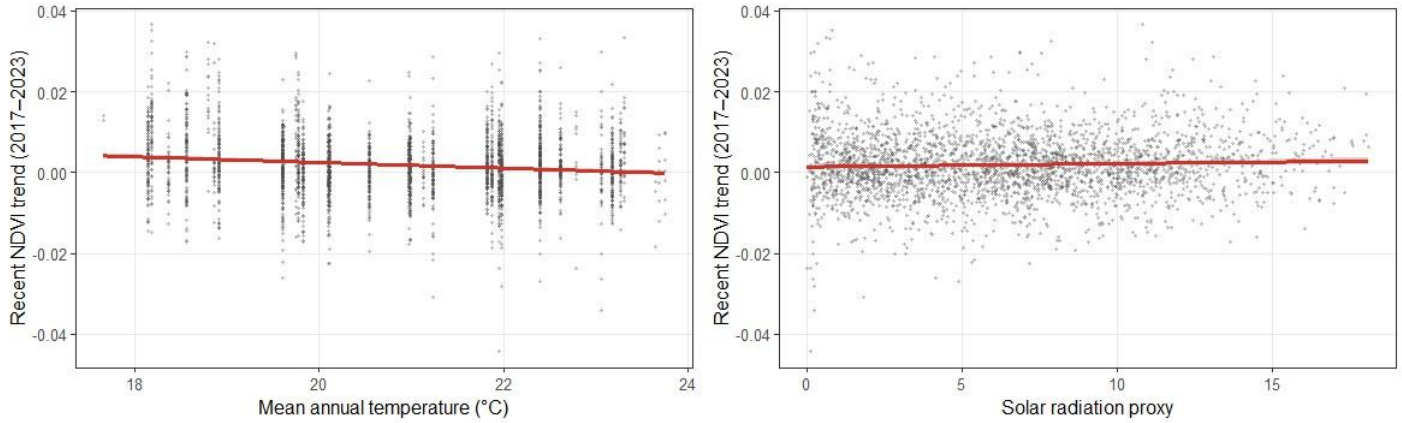

Figure 8: Relationships Between Recent NDVI trends and Topographic Climate Covariates

3.8. Spatial Pattern of Recent NDVI Trends

Spatial pattern of recent NDVI Trends maps shows the spatial distribution of recent NDVI trends (2017-2023) across Sindhuli district. Green points indicate positive trends (increasing vigor), while red points indicate negative trends (decline) [74-76]. The map reveals clear spatial clustering of decline, particularly in the northern and western parts of the district. Positive trends are more scattered and tend to occur in areas with lower solar radiation exposure. Overall, negative trends dominate, consistent with the variable importance and scatterplot results.

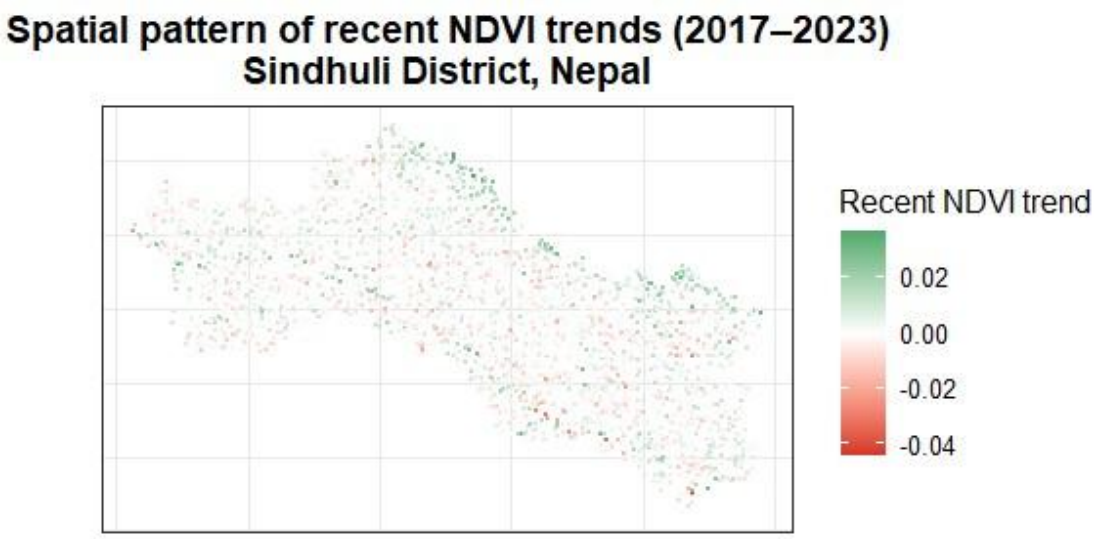

Figure 9: Spatial Pattern of Recent NDVI Trends (2017-2023) Sindhuli Districts, Nepal

3.9. Overall Findings

Taken together, the integrated analysis and results indicate that recent vegetation trend in Sindhuli districts are strongly controlled by topography, especially solar radiation exposure and aspect. Climate covariates (rainfall and temperature) play a secondary but noticeable role [77-80]. These findings provide robust evidence that north and west facing slopes with high solar exposure are most vulnerable to vegetation decline, while south facing slopes show greater stability. These spatial patterns are statistically supported by both linear regression and Random Forest models, confirming solar radiation proxy as the dominant topographic driver. Additionally, exploratory relationships (Supplementary Figure S1) and full regression diagnostics for both the NDVI trend and NDVI mean models (Supplementary Figures S2-S3) are provided in the Supplementary Material.

4. Discussion

4.1. Interpretation of NDVI Trends and Topographic Drivers

The results reveal clear topography driven patterns of vegetation change in Sindhuli district. The NDVI trend map (Figure 4) and change analysis (Figure 5) show that 28.4 % of the district experienced a negative trend and an overall mean decline of -0.04 NDVI units between 2017 and 2023 [81-83]. Decline was consistently concentrated on north and west facing slopes

with high solar radiation proxy values. The inclusion of climate covariates strengthened the models: solar radiation proxy remained the strongest predictor, followed by slope and annual rainfall [84-86]. These findings indicate that increased solar exposure elevates evaporative demand and winter drought stress, while higher rainfall partially mitigates decline. In contrast, south facing slopes exhibited greater stability or slight improvement.

These spatial patterns are statistically supported by both linear regression and Random Forest models, where solar radiation proxy emerged as the strongest predictor of both mean NDVI and NDVI trend. This indicates that increased solar exposure on equator facing slopes likely elevates evaporative demand and winter drought stress, reducing vegetation vigor over time [87-89]. Slope also played a significant secondary role, with steeper terrain associated with more negative trends, probably due to greater runoff and reduced soil moisture retention [90]. These findings align with the well established principle that topography modulates microclimate and water availability in mid hill environments.

4.2. Comparison with Previous Studies

The dominance of solar radiation and aspect as drivers of vegetation decline closely mirrors the results of *Fitzgerald et al. (2023*), who studied a vulnerable population of ***Eucalyptus macrorhyncha*** in South Australia [91-93]. Using hyperspectral imagery and a digital terrain model, they found that solar radiation and aspect explained 68 % of variation in unhealthy vegetation, with northwest facing slopes being most affected. The present study reaches a similar conclusion using freely available MODIS NDVI and SRTM data at the district scale [94-96]. National scale NDVI studies in Nepal have reported mixed greening and browning trends , but they rarely examined topographic controls at the district level. The current analysis fills this gap by providing spatially explicit evidence that topographic position, rather than broad climatic trends alone, strongly shapes vegetation dynamics in the mid hills.

4.3. Implications for Eucolyptus Plantation Management and Local Livelihoods

Sindhuli district contains extensive *Eucalyptus* plantations (***E. camaldulensis*** and ***E. globulus***), which are important sources of fuelwood, poles, and income for rural communities. The observed negative NDVI trends on high solar radiation slopes suggest declining productivity in many plantation areas. The inclusion of rainfall as a covariate shows that drier years exacerbate decline, highlighting the vulnerability of plantations during dry winters [97-100]. A district wide NDVI decline of -0.04 units over seven years may translate to measurable reductions in biomass and fuelwood yield. These findings have practical management implications. Future plantation site selection should prioritise south and southeast facing slopes with lower solar radiation proxy values to improve survival and growth rates [101-103]. Existing plantations on high risk north and west facing slopes may benefit from targeted interventions such as thinning, mulching, or enrichment with native species to reduce water stress. Such site specific planning could enhance the long term economic viability of Eucalyptus plantations and support rural livelihoods while reducing pressure on natural forests.

4.4. Limitations of the Study

This study has several limitations. First, the use of 250 m MODIS NDVI data provides excellent temporal consistency but limits spatial detail. The study is constrained by the spatial resolution of MODIS NDVI, the use of annual composites, and the absence of climate, soil, and anthropogenic covariates[104-106]. At this resolution, pixels often contain a mixture of *Eucalyptus*, other forests, agriculture, and bare land, preventing species specific analysis. Second, although climate covariates (CHIRPS rainfall and ERA5 temperature) were included, soil properties and management practices were not. Third, no field validation was possible due to logistical constraints. Although the statistical models showed acceptable diagnostics, ground truth data would strengthen confidence in the NDVI trend interpretations.

Fourth, the solar radiation proxy is a simplified index; more sophisticated solar radiation models could refine the results. Fifth, the analysis did not incorporate management factors such as planting density, species mixture, or soil properties, which may explain some residual variation [107,108]. Finally, Topographic predictors derived from a 30 m DEM may not fully capture micro terrain effects, and forest mask inaccuracies may influence spatial delineation of NDVI trends. Regression diagnostics indicate minor deviations from model assumptions, and the lack of field validation limits ecological interpretation. Despite these limitations, the integrated remote sensing approach provides a robust district-scale assessment of vegetation dynamics and topographic controls.

4.5. Broader Significance for Sustainable Land Management in Nepal's Mid Hills

Despite these limitations, the study provides the first district scale topographic analysis of vegetation vigor trends in Nepal's mid hills. The open source GEE, QGIS and R workflow developed here is reproducible and can be readily applied to other districts facing similar challenges. The findings highlight the need to integrate topographic considerations into plantation planning and forest management policies. In the context of increasing climate variability, such approaches will be essential for building resilient landscapes and supporting sustainable rural development in the Himalayan mid hills.

5. Conclusion

This study provides the first district scale assessment of long term vegetation vigor and decline in Sindhuli district, Nepal, using MODIS NDVI time series (2017-2023) integrated with SRTM derived topographic variables and climate covariates. The results clearly demonstrate that topography exerts strong control on vegetation dynamics in the mid hills. Negative NDVI trends affected 28.4 % of the district, with decline hotspots concentrated on north and west facing slopes that experience high solar radiation exposure. In contrast, south facing slopes showed greater stability or slight improvement. Statistical modelling confirmed that the solar radiation proxy was the dominant driver of both mean NDVI and NDVI trend, followed by slope.

These findings highlight that solar exposure and terrain steepness are primary factors influencing vegetation stress and decline in this topographically complex landscape. The observed vegetation decline has direct implications for the management of *Eucalyptus* plantations, which form a significant part of Sindhuli's rural landscape and economy. To improve long term productivity and resilience, future plantation establishment should prioritise south and southeast facing slopes with lower solar radiation proxy values. Existing plantations on high risk north and west facing slopes may require targeted interventions such as reduced planting density, mulching, or gradual conversion to mixed native exotic systems. District level forest offices and community forestry groups should incorporate topographic suitability maps into plantation planning.

At the national level, these results support the integration of remote sensing based topographic analysis into Nepal's forest management and climate adaptation policies, helping to safeguard rural livelihoods and reduce pressure on natural forests. Future studies should extend this approach to other mid hill districts and incorporate higher resolution Sentinel-2 data once improved cloud masking techniques are applied. Field validation of NDVI trends and species specific mapping (particularly *E. globulus* and *E. camaldulensis*) would strengthen the findings. Additional environmental and management variables such as soil properties, plantation age, and local land use practices should be included to explain residual variation. Finally, linking NDVI based vigor trends to quantitative estimates of biomass productivity and economic losses would provide stronger evidence for policy and investment decisions in sustainable plantation forestry.

In summary, this research demonstrates that topography driven vegetation decline is an important but often overlooked factor in Nepal's mid hills. The open source workflow developed here offers a practical and scalable tool for monitoring and managing vegetation resources under changing climatic conditions.

Supplementary Material

Supplementary Figure S1 Between Mean NDVI and Solar Radiation Proxy

Scatterplot illustrating the bivariate relationship between mean NDVI and the solar radiation proxy. Each point represents a sampled pixel, and the fitted regression line with confidence interval highlights the slight positive association between vegetation vigor and solar exposure.

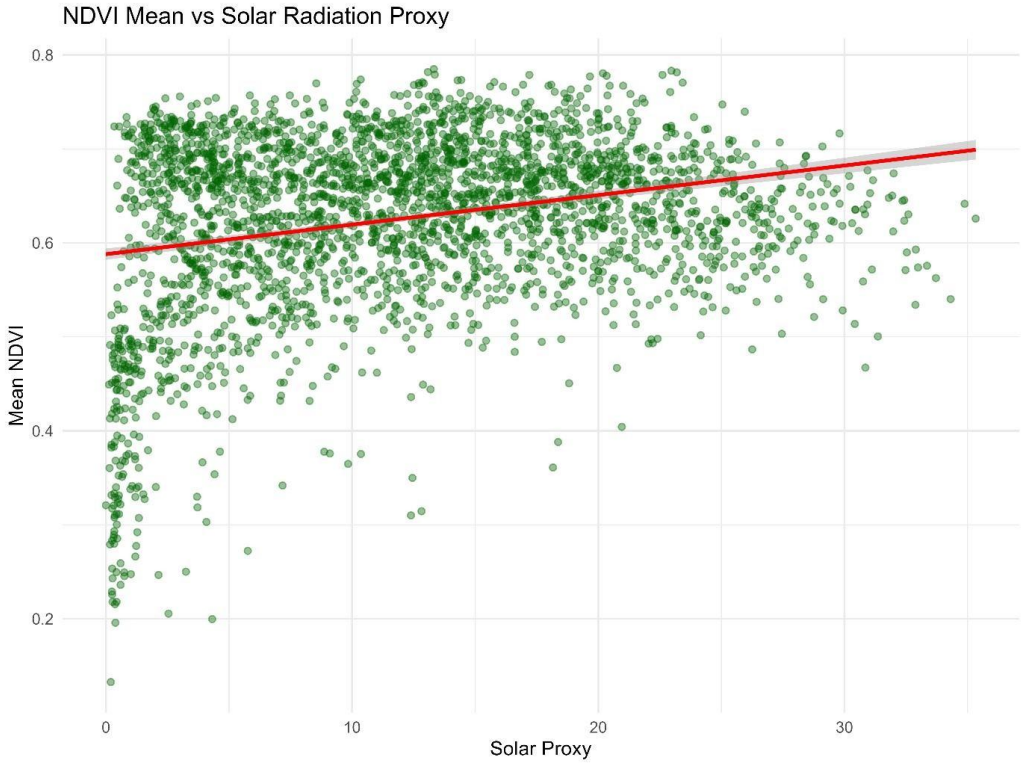

Figure 10: NDVI Mean vs Solar Radiation Proxy

Supplementary Figure S2. Diagnostic Plots for the NDVI Trend Regression Model

Four diagnostic panels evaluating model assumptions: (A) residuals vs. fitted values, (B) Q-Q residuals, (C) scale location plot, and (D) residuals vs. leverage with Cook's distance contours. These diagnostics confirm acceptable normality, variance structure, and influence patterns for the NDVI trend model.

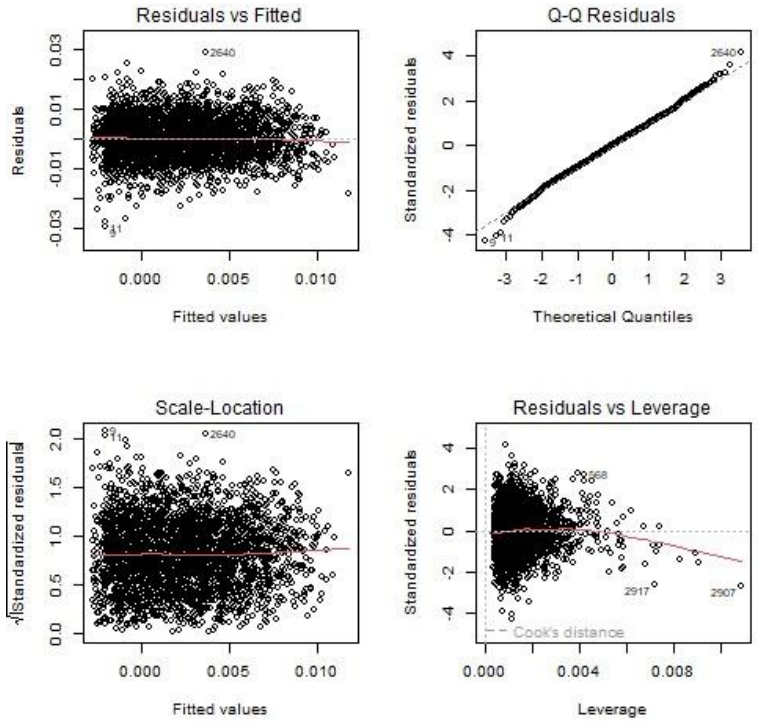

Figure 11: Diagnostic Plots for the NDVI Trend Regression Model

Supplementary Figure S3. Diagnostic Plots for the NDVI Mean Regression Model: Diagnostic plots assessing linearity, residual distribution, homoscedasticity, and influential observations for the NDVI mean model. The diagnostics indicate that the model is statistically robust and suitable for interpreting the relationship between mean NDVI and topographic predictors.

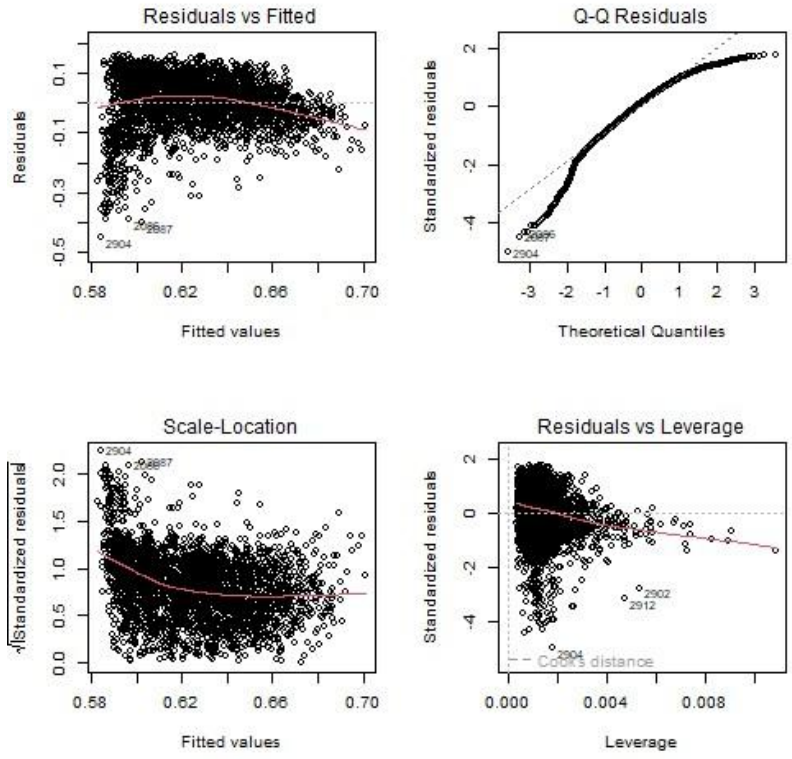

Figure 12: Diagnostic Plots for the NDVI Mean Regression Model

Author Contributions:

Conceptualization, methodology, software, validation, formal analysis, investigation, data curation, writing original draft preparation, writing review and editing, visualization, and project administration: P.G. (Prabin Gauli). The author has read and agreed to the published version of the manuscript.

Funding:

This research received no external funding.

Data Availability Statement:

The MODIS MOD13Q1 NDVI data used in this study are publicly available from NASA

EOSDIS Land Processes DAAC. The SRTM 90 m DEM is available from the CGIAR-CSI

SRTM database. The administrative boundary of Sindhuli district was obtained from the

Chuche Naksa dataset of the Government of Nepal. All processed data, GEE scripts, QGIand R code generated during the study are available from the corresponding author upon reasonable request.

Acknowledgments:

The author also acknowledges the open access data providers (NASA MODIS, CGIAR-CSI SRTM, and Google Earth Engine) that made this study possible without additional cost.

Conflicts of Interest:

The author declares no conflicts of interest.

References

1. Allen, C. D., Macalady, A. K., Chenchouni, H., Bachelet, D., McDowell, N., et al. (2010). A global overview of drought and heat-induced tree mortality reveals emerging climate change risks for forests. *Forest Ecology and Management, 259*(4), 660–684.
2. Hammond, W. M., Williams, A. P., Abatzoglou, J. T., Adams, H. D., Klein, T., et al. (2022). Global field observations of tree die-off reveal hotter-drought fingerprint for Earth's forests. *Nature Communications, 13*, Article 1761.
3. Choat, B., Brodribb, T. J., Brodersen, C. R., Duursma, R. A., López, R., et al. (2018). Triggers of tree mortality under drought. *Nature, 558*(7711), 531–539.
4. Jump, A. S., Ruiz-Benito, P., Greenwood, S., Allen, C. D., Kitzberger, T., et al. (2017). Structural overshoot of tree growth with climate variability and the global spectrum of drought-induced forest dieback. *Global Change Biology, 23*(9), 3742–3757.
5. Hawthorne, S., & Miniat, C. F. (2018). Topography may mitigate drought effects on vegetation along a hillslope gradient. *Ecohydrology, 11*(1), Article e1825.
6. Moeslund, J. E., Arge, L., Bøcher, P. K., Dalgaard, T., & Svenning, J.-C. (2013). Topography as a driver of local terrestrial vascular plant diversity patterns. *Nordic Journal of Botany, 31*(2), 129–144.
7. Auslander, M., Nevo, E., & Inbar, M. (2003). The effects of slope orientation on plant growth, developmental instability and susceptibility to herbivores. *Journal of Arid Environments, 55*(3), 405–416.
8. Tian, H., Melillo, J. M., Kicklighter, D. W., McGuire, A. D., & Helfrich, J. (2001). Regional carbon dynamics in monsoon Asia and its implications for the global carbon cycle. *Global and Planetary Change, 31*(1–4), 109–124.
9. Baniya, B., Tang, Q., Huang, Z., Sun, S., & Techato, K. (2018). Spatial and temporal variation of NDVI in response to climate change and the implication for carbon dynamics in Nepal. *Forests, 9*(6), Article 329.
10. Krakauer, N. Y., Lakhankar, T., & Anadón, J. D. (2017). Mapping and attributing normalized difference vegetation index trends for Nepal. *Remote Sensing, 9*(10), Article 986.
11. Nila, S., Bhardwaj, A., & Joshi, R. (2025). Spatiotemporal vegetation dynamics in the Hindu Kush Himalayan region using MODIS NDVI time series. *Environmental Monitoring and Assessment, 197*, Article 234.
12. Paudel, B., Zhang, Y., Li, S., & Liu, L. (2022). Spatiotemporal patterns of vegetation greenness change and associated climatic drivers in the Hindu Kush Himalayan region. *Ecological Indicators, 144*, Article 109453.
13. Gurung, A., Bista, R., Karki, R., Shrestha, S., Uprety, D., et al. (2019). Community-based forest management and its role in improving forest conditions and livelihoods in Nepal's mid-hills. *Journal of Forest Research, 24*(3), 159–167.
14. Pandit, R., Neupane, P. R., & Wagle, B. H. (2021). Economics of Eucalyptus plantation in the eastern Terai of Nepal. *Banko Janakari, 31*(1), 23–31.
15. K.C., A., Paudel, N. S., & Ojha, H. (2023). Declining productivity of Eucalyptus plantations in the mid-hills of Nepal: Farmers' perceptions and management challenges. *Journal of Forest and Livelihood, 22*(1), 45–58.
16. Pettorelli, N., Vik, J. O., Mysterud, A., Gaillard, J.-M., Tucker, C. J., et al. (2005). Using the satellite-derived NDVI to assess ecological responses to environmental change. *Trends in Ecology & Evolution, 20*(9), 503–510.
17. Huang, S., Tang, L., Hupy, J. P., Wang, Y., & Shao, G. (2021). A commentary review on the use of normalized difference vegetation index (NDVI) in the era of popular remote sensing. *Journal of Forestry Research, 32*(1), 1–6.
18. Fitzgerald, D. L., Peters, S., Guerin, G. R., McGrath, A., & Keppel, G. (2023). Quantifying dieback in a vulnerable population of Eucalyptus macrorhyncha using remote sensing. *Land, 12*(7), Article 1271.
19. Tucker, C. J. (1979). Red and photographic infrared linear combinations for monitoring vegetation. *Remote Sensing of Environment, 8*(2), 127–150.
20. Huete, A., Didan, K., Miura, T., Rodriguez, E. P., Gao, X., et al. (2002). Overview of the radiometric and biophysical performance of the MODIS vegetation indices. *Remote Sensing of Environment, 83*(1–2), 195–213.
21. Didan, K. (2015). *MOD13Q1 MODIS/Terra vegetation indices 16-day L3 global 250 m SIN grid V006* [Data set]. NASA EOSDIS Land Processes DAAC.
22. Verbesselt, J., Hyndman, R., Newnham, G., & Culvenor, D. (2010). Detecting trend and seasonal changes in satellite

image time series. *Remote Sensing of Environment, 114*(1), 106–115.
23. Zhang, X., Friedl, M. A., & Schaaf, C. B. (2003). Monitoring vegetation phenology using MODIS. *Remote Sensing of Environment, 84*(3), 471–475.
24. Jiang, Z., Huete, A. R., Didan, K., & Miura, T. (2008). Development of a two-band enhanced vegetation index without a blue band. *Remote Sensing of Environment, 112*(10), 3833–3845.
25. Fensholt, R., & Proud, S. R. (2012). Evaluation of earth observation-based global long-term vegetation trends: Comparing GIMMS and MODIS global NDVI time series. *Remote Sensing of Environment, 119*, 131–147.
26. Forkel, M., Carvalhais, N., Verbesselt, J., Mahecha, M. D., Neigh, C. S. R., et al. (2013). Trend change detection in NDVI time series: Effects of inter-annual variability and methodology. *Remote Sensing, 5*(5), 2113–2144.
27. Tian, F., Fensholt, R., Verbesselt, J., Grogan, K., Horion, S., & Wang, Y. (2015). Evaluating temporal consistency of long-term global NDVI datasets for trend analysis. *Remote Sensing of Environment, 163*, 326–340.
28. Eastman, J. R., Sangermano, F., Machado, E. A., Rogan, J., & Anyamba, A. (2013). Global trends in seasonality of normalized difference vegetation index (NDVI), 1982–2011. *Remote Sensing, 5*(10), 4799–4818.
29. De Jong, R., De Bruin, S., De Wit, A., Schaepman, M. E., & Dent, D. L. (2011). Analysis of monotonic greening and browning trends from global NDVI time-series. *Remote Sensing of Environment, 115*(2), 692–702.
30. Shrestha, B., Zhang, L., Shrestha, S., & Khadka, N. (2024). Spatiotemporal patterns, sustainability, and primary drivers of NDVI-derived vegetation dynamics (2003–2022) in Nepal. *Environmental Monitoring and Assessment, 196*, Article 607.
31. Mishra, N. B., & Mainali, K. P. (2017). Greening and browning of the Himalaya: Spatial patterns and the role of climatic change and human drivers. *Science of the Total Environment*, 587–588, 326–339.
32. Uddin, K., Shrestha, H. L., Murthy, M. S. R., Bajracharya, B., Shrestha, B., et al. (2015). Development of 2010 national land cover database for Nepal. *Journal of Environmental Management, 148*, 82–90.
33. Department of Forest Research and Survey (DFRS). (2015). *State of Nepal's forests*. Government of Nepal.
34. Panday, P. K., & Ghimire, B. (2012). Time-series analysis of NDVI from AVHRR data over the Hindu Kush–Himalayan region for the period 1982–2006. *International Journal of Remote Sensing, 33*(21), 6710–6728.
35. Poudel, K. P., Temesgen, H., & Gray, A. N. (2015). Estimating forest aboveground biomass using LiDAR and Landsat data in the Pacific Northwest, USA. *Forest Ecology and Management, 335*, 44–55.
36. Bhuyan, M., Singh, B., Vid, S., & Jeganathan, C. (2022). Analysing the spatio-temporal patterns of vegetation dynamics and their responses to climatic parameters in Meghalaya from 2001 to 2020. *Environmental Monitoring and Assessment, 195*, Article 94.
37. Guo, W., Liu, H., & Anenkhonov, O. A. (2021). Vegetation cover changes and their relationship with climate in the forest-steppe ecotone of the Selenga River basin. *Journal of Arid Land, 13*(5), 455–469.
38. Anderson, K., Fawcett, D., Cugulliere, A., Benford, S., Jones, D., et al. (2020). Vegetation expansion in the subnival Hindu Kush Himalaya. *Global Change Biology, 26*(3), 1608–1625.
39. Pandey, S., Poudyal, B. H., & Maraseni, T. (2021). Climate change impacts and adaptation strategies in the Hindu Kush Himalaya: A review. *Environmental Science & Policy, 124*, 254–265.
40. Kandel, P., Gurung, J., Chettri, N., Ning, W., & Sharma, E. (2016). Biodiversity research trends and gap analysis from a transboundary landscape, Eastern Himalayas. *Journal of Asia-Pacific Biodiversity, 9*(1), 1–10.
41. Wilson, J. P., & Gallant, J. C. (Eds.). (2000). *Terrain analysis: Principles and applications*. Wiley.
42. Moore, I. D., Grayson, R. B., & Ladson, A. R. (1991). Digital terrain modeling: A review of hydrological, geomorphological, and biological applications. *Hydrological Processes, 5*(1), 3–30.
43. Fu, P., & Rich, P. M. (2002). A geometric solar radiation model with applications in agriculture and forestry. *Computers and Electronics in Agriculture, 37*(1–3), 25–35.
44. Pierce, K. B., Jr., Lookingbill, T., & Urban, D. (2005). A simple method for estimating potential relative radiation (PRR) for landscape-vegetation analysis. *Landscape Ecology, 20*(2), 137–147.
45. Dobrowski, S. Z. (2011). A climatic basis for microrefugia: The influence of terrain on climate. *Global Change Biology, 17*(2), 1022–1035.
46. Bennie, J., Huntley, B., Wiltshire, A., Hill, M. O., & Baxter, R. (2008). Slope, aspect and climate: Spatially explicit and implicit models of topographic microclimate in chalk grassland. *Ecological Modelling, 216*(1), 47–59.
47. McCune, B., & Keon, D. (2002). Equations for potential annual direct incident radiation and heat load. *Journal of Vegetation Science, 1*3(4), 603–606.
48. Griffiths, R. P., Madritch, M. D., & Swanson, A. K. (2009). The effects of topography on forest soil characteristics in the Oregon Cascade Mountains (USA): Implications for the effects of climate change on soil properties. *Forest Ecology and Management, 257*(1), 1–7.
49. Florinsky, I. V., & Kuryakova, G. A. (1996). Influence of topography on some vegetation cover properties. *Catena, 27*(2), 123–141.
50. Tateno, R., & Takeda, H. (2003). Forest structure and tree species distribution in relation to topography-mediated heterogeneity of soil nitrogen and light at the forest floor. *Ecological Research, 18*(5), 559–571.
51. Band, L. E., Patterson, P., Nemani, R., & Running, S. W. (1993). Forest ecosystem processes at the watershed scale: Incorporating hillslope hydrology. *Agricultural and Forest Meteorology, 63*(1–2), 93–126.
52. Kumar, L., Skidmore, A. K., & Knowles, E. (1997). Modelling topographic variation in solar radiation in a GIS environment.

International Journal of Geographical Information Science, 11(5), 475–497.
53. Khanal, S. N. *Eucalyptus plantations in Nepal*. Food and Agriculture Organization of the United Nations.
54. Pokhrel, M. (2025). In Nepal, a eucalyptus boom became an ecological cautionary tale. *Mongabay*.
55. Dhakal, A. (2008). *Tree growth performance in private plantations in Nepal's central Terai region* (Master's thesis, University of Southern Queensland).
56. White, K. J. (1985). *Eucalyptus species trials and plantations at Sagarnath, Nepal*. Sagarnath Forest Development Project.
57. Gilmour, D. A., & Fisher, R. J. (1991). *Villagers, forests and foresters: The philosophy, process and practice of community forestry in Nepal*. Sahayogi Press.
58. Jackson, J. K. (1994). *Manual of afforestation in Nepal* (2nd ed.). Forest Research and Survey Centre.
59. Pandey, D., & Brown, C. (2000). Teak: A global overview. *Unasylva, 51*(201), 3–13.
60. Arnold, J. E. M., & Dewees, P. A. (Eds.). (1997). *Farms, trees and farmers: Responses to agricultural intensification*. Earthscan Publications.
61. Saxena, N. C. (1997). The saga of participatory forest management in India. Center for International Forestry Research.
62. Byron, N., & Arnold, M. (1999). What futures for the people of the tropical forests? *World Development, 27*(5), 789–805.
63. Breiman, L. (2001). Random forests. *Machine Learning, 45*(1), 5–32.
64. Cutler, D. R., Edwards, T. C., Beard, K. H., Cutler, A., Hess, K. T., et al. (2007). Random forests for classification in ecology. *Ecology, 88*(11), 2783–2792.
65. Friedman, J. H. (2001). Greedy function approximation: A gradient boosting machine. *Annals of Statistics, 29*(5), 1189–1232.
66. Hijmans, R. J. (2023). *raster: Geographic data analysis and modeling* (Version 3.5-15) [R package].
67. Pebesma, E. (2018). Simple features for R: Standardized support for spatial vector data. *The R Journal, 10*(1), 439–446.
68. Liaw, A., & Wiener, M. (2002). Classification and regression by randomForest. *R News, 2*(3), 18–22.
69. Kuhn, M. (2008). Building predictive models in R using the caret package. *Journal of Statistical Software, 28*(5), 1–26.
70. Evans, J. S., & Murphy, M. A. (2022). *spatialEco: Spatial analysis and modelling utilities* (Version 1.3-7) [R package].
71. James, G., Witten, D., Hastie, T., & Tibshirani, R. (2021). *An introduction to statistical learning: With applications in R* (2nd ed.). Springer.
72. Strobl, C., Boulesteix, A.-L., Zeileis, A., & Hothorn, T. (2007). Bias in random forest variable importance measures: Illustrations, sources and a solution. *BMC Bioinformatics, 8*, Article 25.
73. Prasad, A. M., Iverson, L. R., & Liaw, A. (2006). Newer classification and regression tree techniques: Bagging and random forests for ecological prediction. *Ecosystems, 9*(2), 181–199.
74. Elith, J., Leathwick, J. R., & Hastie, T. (2008). A working guide to boosted regression trees. *Journal of Animal Ecology, 77*(4), 802–813.
75. Akaike, H. (1974). A new look at the statistical model identification. *IEEE Transactions on Automatic Control, 19*(6), 716–723.
76. Burnham, K. P., & Anderson, D. R. (2002). *Model selection and multimodel inference: A practical information-theoretic approach* (2nd ed.). Springer.
77. Hothorn, T., Hornik, K., & Zeileis, A. (2006). Unbiased recursive partitioning: A conditional inference framework. *Journal of Computational and Graphical Statistics, 15*(3), 651–674.
78. QGIS Development Team. (2023). *QGIS Geographic Information System* [Computer software]. Open Source Geospatial Foundation.
79. Esri. (2023). *ArcGIS Pro* (Version 3.x) [Computer software]. Environmental Systems Research Institute.
80. Zanaga, D., Van De Kerchove, R., De Keersmaecker, W., Souverijns, N., Scholte, R., et al. (2021). *ESA WorldCover 10 m 2020 v100* [Data set]. Zenodo.
81. Farr, T. G., Rosen, P. A., Caro, E., Crippen, R., Duren, R., et al. (2007). The Shuttle Radar Topography Mission. *Reviews of Geophysics, 45*(2), Article RG2004.
82. Gorelick, N., Hancher, M., Dixon, M., Ilyushchenko, S., Thau, D., et al. (2017). Google Earth Engine: Planetary-scale geospatial analysis for everyone. *Remote Sensing of Environment, 202*, 18–27.
83. Wickham, H. (2016). *ggplot2: Elegant graphics for data analysis* (2nd ed.). Springer.
84. Hijmans, R. J. (2023). *terra: Spatial data analysis* (Version 1.7-29) [R package].
85. R Core Team. (2023). *R: A language and environment for statistical computing* (Version 4.3). R Foundation for Statistical Computing.
86. Dunnington, D. (2023). *ggspatial: Spatial data framework for ggplot2* (Version 1.1.9) [R package].
87. R Core Team. (2020). *R: A language and environment for statistical computing*. R Foundation for Statistical Computing.
88. Jarvis, A., Reuter, H. I., Nelson, A., & Guevara, E. (2008). *Hole-filled SRTM for the globe Version 4*. CGIAR-CSI SRTM 90m Database.
89. Bivand, R. S., Pebesma, E., & Gomez-Rubio, V. (2013). *Applied spatial data analysis with R* (2nd ed.). Springer.
90. Hengl, T., & Reuter, H. I. (Eds.). (2009). *Geomorphometry: Concepts, software, applications*. Elsevier.
91. Neteler, M., & Mitasova, H. (2008). *Open source GIS: A GRASS GIS approach* (3rd ed.). Springer.
92. Anderegg, W. R. L., Kane, J. M., & Anderegg, L. D. L. (2013). Consequences of widespread tree mortality triggered by drought and temperature stress. *Nature Climate Change, 3*(1), 30–36.
93. Breshears, D. D., Cobb, N. S., Rich, P. M., Price, K. P., Allen, C. D., et al. (2005). Regional vegetation die-off in response to global-change-type drought. *Proceedings of the National Academy of Sciences, 102*(42), 15144–15148.
94. McDowell, N. G., Pockman, W. T., Allen, C. D., Breshears,

D. D., Cobb, N., Kolb, T., et al. (2008). Mechanisms of plant survival and mortality during drought: Why do some plants survive while others succumb to drought? *New Phytologist, 178*(4), 719–739.

95. Adams, H. D., Guardiola-Claramonte, M., Barron-Gafford, G. A., Villegas, J. C., Breshears, D. D., et al. (2009). Temperature sensitivity of drought-induced tree mortality portends increased regional die-off under global-change-type drought. *Proceedings of the National Academy of Sciences, 106*(17), 7063–7066.
96. Williams, A. P., Allen, C. D., Macalady, A. K., Griffin, D., Woodhouse, C. A., et al. (2013). Temperature as a potent driver of regional forest drought stress and tree mortality. *Nature Climate Change, 3*(3), 292–297.
97. Gautam, A. P., Webb, E. L., & Eiumnoh, A. (2002). GIS assessment of land use/land cover changes associated with community forestry implementation in the Middle Hills of Nepal. *Mountain Research and Development, 22*(1), 63–69.
98. Gautam, A. P., Webb, E. L., Shivakoti, G. P., & Zoebisch, M. A. (2003). Land use dynamics and landscape change pattern in a mountain watershed in Nepal. *Agriculture, Ecosystems & Environment, 99*(1–3), 83–96.
99. Fox, J. (1993). Forest resources in a Nepali village in 1980 and 1990: The positive influence of population growth. *Mountain Research and Development, 13*(1), 89–98.
100. Jackson, W. J., Tamrakar, R. M., Hunt, S., & Shepherd, K. R. (1998). Land-use changes in two Middle Hills districts of Nepal. *Mountain Research and Development, 18*(3), 193–212.
101. Virgo, K. J., & Subba, K. J. (1994). Land-use change between 1978 and 1990 in Dhankuta district, Koshi Hills, eastern Nepal. *Mountain Research and Development, 14*(2), 159–170.
102. Thapa, G. B., & Weber, K. E. (1995). Natural resource degradation in a small watershed in Nepal: Complex causes and remedial measures. *Natural Resources Forum, 19*(4), 285–296.
103. Schmidt-Vogt, D. (1998). Defining degraded forest in the Middle Hills of Nepal. *Banko Janakari, 8*(1), 19–22.
104. Shrestha, B. M. (1999). *The role of community forestry in the rehabilitation of degraded hills in Nepal* (Doctoral dissertation, University of Reading).
105. Branney, P., & Yadav, K. P. (1998). *Changes in community forest condition and management 1994–1998: Analysis of information from the Forest Resource Assessment Study and Socio-economic Study in the Koshi Hills. Nepal-UK Community Forestry Project*.
106. Acharya, K. P. (2002). Twenty-four years of community forestry in Nepal. *International Forestry Review, 4*(2), 149–156.
107. Malla, Y. B. (2001). Changing policies and the persistence of patron-client relations in Nepal: Stakeholders' responses to changes in forest policies. *Environmental History, 6*(2), 287–307.
108. Ojha, H. R., Cameron, J., & Kumar, C. (2009). Deliberation or symbolic violence? The governance of community forestry in Nepal. *Forest Policy and Economics, 11*(5–6), 365–374.